ACS APPLIED MATERIALS & INTERFACES

www.acsami.org

Research Article

Chemically Coupled Interfacial Adhesion in Multimaterial Printing of Hydrogels and Elastomers

Kevin Tian, Zhigang Suo,* and Joost J. Vlassak*

Cite This: *ACS Appl. Mater. Interfaces* 2020, 12, 31002–31009

Read Online

ACCESS | Metrics & More | Article Recommendations | Supporting Information

ABSTRACT: Functional devices that use hydrogels as ionic conductors and elastomers as dielectrics have the advantage of being soft, stretchable, transparent, and biocompatible, making them ideal for biomedical applications. These devices are typically fabricated by manual assembly. Techniques for the manufacturing of soft materials have generally not looked at integrating multiple dissimilar materials. Silane coupling agents have recently shown promise for creating strong bonds between hydrogels and elastomers but have yet to be used in the extrusion printing of complex devices that integrate both hydrogels and elastomers. Here, we demonstrate the viability of silane coupling agents in a system with the rheology and functional composition necessary for three-dimensional (3D) extrusion printing of hydrogel–elastomer materials, specifically polyacrylamide (PAAm) hydrogel and poly(dimethylsiloxane) (PDMS) hydrophobic elastomer. By introducing a charge-neutral surfactant in the PDMS and adjusting silane concentrations in the PAAm, cast material samples demonstrate strong adhesion. We were also able to achieve an interfacial toughness of up to $\Gamma = 193 \pm 6.3$ J/m^2 for a fully extrusion printed PAAm hydrogel-on-PDMS bilayer. This result demonstrates that an integration strategy based on silane coupling agents makes it possible for extrusion printing of a wide variety of hydrogel and silicone elastomers.

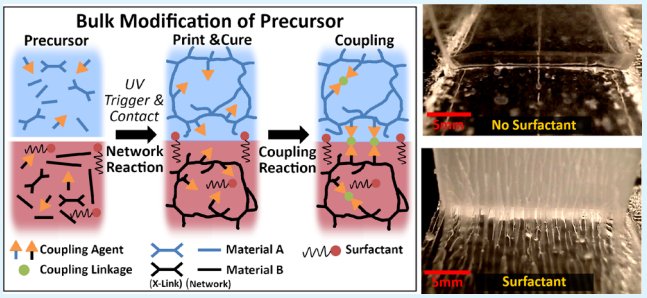

KEYWORDS: *3D extrusion printing, 3DP, hydrogel, elastomer, PDMS, ionotronics, interfacial adhesion, silane coupling*

INTRODUCTION

As the field of stretchable electronics matures, functional devices that use hydrogels as ionic conductors and elastomers as dielectrics show great promise in applications that require softness, stretchability, transparency, and biocompatability.[1] However, only recently have developments been made toward the advanced manufacture of heterogeneous soft material devices. Prior to these developments, casting and manual assembly were the dominant means of making these devices, which include skin-like sensors,[2−5] ionic cables,[6] optical waveguides,[7] touch panels,[8] actuators,[9] and electroluminescent sources.[3,10] Some studies have begun moving beyond manual assembly by combining casting with other techniques like sewing.[11,12] In terms of single-step processes, a variety of manufacturing techniques have been applied toward hydrogel device fabrication, including stereolithography,[13] two-photon polymerization,[14] and inkjet printing.[15,16] Material extrusion, also known as extrusion printing,[17] three-dimensional (3D) plotting,[18] and direct ink writing,[19] has the advantages of technological simplicity, ease of adopting multiple materials, and low commercial cost.[20]

Multimaterial printing, or the concurrent printing of dissimilar materials, is an important technique because it allows fabrication of devices with the most functionality. In the same way that electrical circuitry relies on dissimilar materials to function, hydrogel-based devices require the integration of hydrogels with elastomers, both hydrophilic and hydrophobic. Without proper integration, the devices could be prone to failures such as delamination and their long-term reliability may be questionable. Although there are abundance of studies that have looked at the extrusion printing of soft materials independently, including hydrogels[21−28] and silicone elastomers,[29−36] far fewer have looked at combined hydrogel–elastomer device fabrication.[37−39]

Integration techniques in hydrogel–elastomer fabrication studies are generally divided into two categories, physical and chemical, depending on the type of bond that is formed between the hydrogel and elastomer. Techniques that rely on physical bonds for adhesion, such as hydrogen bonding[40,41] or contact forces from conformation,[3,39,42,43] may result in acceptable devices but rely on the lack of significant driving forces to prevent delamination. Strong integration, which is generally indicated by cohesive failure, has yet to be

Received: April 23, 2020
Accepted: June 15, 2020
Published: June 15, 2020

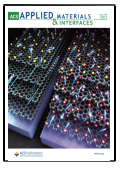

https://dx.doi.org/10.1021/acsami.0c07468
ACS Appl. Mater. Interfaces 2020, 12, 31002–31009

demonstrated between hydrogel and elastomer through physical bonds. Techniques utilizing chemical bonds between hydrogels and elastomers for their integration are based predominantly on the UV photo-initiator benzophenone, with the majority relying on surface modifications[44−46] and one instance of volume modification.[37] These techniques use a compound that upon UV exposure generates free radicals capable of reacting with both the hydrogel and elastomer networks to form chemical cross-links between them. In these techniques, integration of the two materials occurs simultaneously with network formation. Silane-based chemical coupling has also been successfully demonstrated for hydrogels and elastomers.[12,38] In this approach, a compatible silane coupling agent is copolymerized with the bulk hydrogel or elastomer and allowed to react independently of the polymerization reaction (Figure 1). Previous work using silane coupling agents with hydrogels did not explore its viability within the extrusion printing context, as a precursor with a silane coupling agent and a rheology appropriate for extrusion printing was not developed. Furthermore, the system must be adapted for hydrogels of high ionic strength to be relevant for ionotronic applications. Since silane coupling represents a different pathway toward achieving dissimilar material integration for extrusion 3D printing, validating its viability is worth exploring.

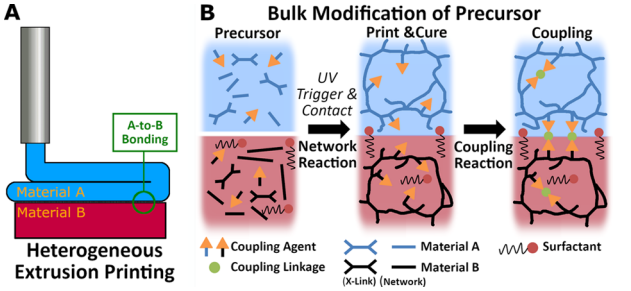

Figure 1. (A) In heterogeneous printing, one must account for the integration of materials across material interfaces, particularly as one material is printed onto another. B) We highlight the use of coupling agents that can be integrated into the bulk of the materials being printed, but can subsequently bond across the material interface even after the networks have been formed.

This work studies the viability of silane coupling agents as a strategy for adhesion enhancement for the extrusion 3D printing of high ionic strength hydrogels and silicone elastomers. Polyacrylamide (PAAm) hydrogel and poly(dimethylsiloxane) (PDMS) hydrophobic elastomer were selected as a model system for their simplicity, ease of fabrication, and ubiquity in hydrogel ionotronic devices. As the foundation for the extrusion printability of these materials, we build upon existing work in the extrusion 3D-printing context.[40]

METHODS

Figure 2 highlights the various chemical reactions that underlie the silane-based coupling agent strategy we have employed. Because of the maturity of the silane chemistry, there exists a library of commercially available compounds.[47,48] As a result, the strategy can be used for a wide variety of networks. In this study, we selected 3-(tri-methoxy-silyl)propylmethacrylate (TMSPMA) and tri-ethoxy-vinylsilane (TEOVS) as the coupling agents for the PAAm hydrogel and PDMS networks, respectively. Co-polymerizing these agents into their respective networks (Figure 2) effectively modifies the networks to be capable of coupling. The hydrolysis step activates the silane compounds by converting methyl groups into hydroxyl groups, a process that occurs more readily under acidic conditions.[49] It is vital to note that this step readily occurs in the hydrogel due to its high water content, provided the pH is sufficiently low (nominally below pH 3.0).[49] Hydrolysis does not, however, occur naturally within the PDMS elastomer[38] because of the low availability of water. Hydrolysis in the PDMS can be initiated by making contact with acidic water or with a hydrogel, effectively a surface-localized activation of the silane coupling agent. It is important to note that condensation is a reaction that readily occurs under neutral to high pH conditions, with significantly reduced kinetics at low pH;[49] to preserve condensation sites during processing but still maintain a reasonable rate of condensation during curing, the pH was tuned to 3.5 and was not otherwise modified.

The requirement to couple both networks is not sufficient for successful extrusion printing, and several other factors need to be addressed. Wetting is critical for the printability of a material in the extrusion printing process. Previous studies have indicated that integrating surfactants into the PDMS is a viable strategy for improving wetting behaviors.[50−52] Integrating surfactants into the

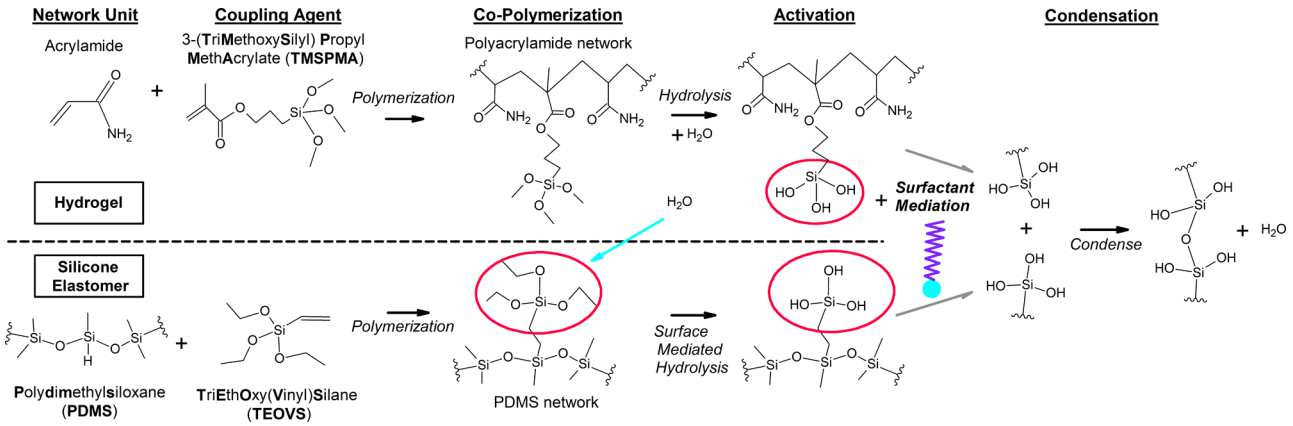

Figure 2. Schematic of the chemical reactions for the incorporation of coupling agents into hydrogel and silicone elastomer networks and their subsequent activity leading to material integration. Coupling agents are incorporated into their network through reactions with the network unit. After copolymerization into the network, the coupling agents undergo activation via hydrolysis; this process readily occurs in the hydrogel but requires mediation with water (at the hydrogel surface) to occur in the PDMS. After activation, the coupling agents are able to condense across the material interface to form chemical linkages between the two networks.

https://dx.doi.org/10.1021/acsami.0c07468
ACS Appl. Mater. Interfaces 2020, 12, 31002−31009

bulk may also accelerate the coupling reaction and achieve satisfactory wetting behavior without the need for additional processing such as plasma oxidation.[40] In line with previous work, we opt to integrate the surfactant into the PDMS, though integration into the hydrogel precursor is also possible. To avoid incompatibilities due to the high ionic strength of the hydrogel precursor, a noncharged surfactant was selected for use (BrijL23). In order for the surfactant to affect the silane condensation, the surfactant must migrate to the surface on a faster time scale than the hydrogel and PDMS network formation. For the selected surfactant concentration, the water contact angle drops by 20° within 10 min and is estimated to proceed over the course of 1 h.[52] This is fast relative to polyacrylamide[53] and UV-curable PDMS network formation, which is fastest during and shortly after UV exposure (approximately 1 h) and continues over the course of more than 8 h. PDMS reaction time was estimated based on information provided by the manufacturer.

The hydrogel precursor formulation as described by Tian et al.[40] contains lithium chloride (LiCl) salt for its conductive and hygroscopic properties and uncross-linked PAAm chains for rheological modification. The materials used in this study have been modified from this formula to incorporate the silane coupling agents and other necessary compounds. The rheological properties of the modifier are suitable for printing and differ minimally from those observed previously for the same concentration of polymer in an aqueous solution (see the Supporting Information Figure S1).[40] Samples for initial testing were fabricated using casting rather than printing for throughput and experimental reasons. Though clear differences exist, a previous study has supported the idea that the underlying mechanisms of adhesion are not expected to differ significantly beyond shear-induced printing effects on the material properties.[41]

In particular, we highlight the role of several compounds in the hydrogel and PDMS elastomer. In the hydrogel precursor, TMSPMA serves as the coupling agent. Acetic acid is used to adjust the pH of the precursor to 3.5 to control hydrolysis/condensation.[38,49] Because the reaction kinetics of the silane coupling agents are sensitive to pH and the UV curing rate is tied to initiator concentration, the UV initiator was changed from α-ketoglutaric acid to Irgacure 2959 to avoid coupling the pH to the curing rate. In the PDMS precursor, TEOVS serves as the coupling agent; BrijL23 acts as the surfactant (chemical name: poly(oxyethylene)(23) lauryl ether, $CH_3(CH_2)_{10}CH_2(OCH_2CH_2)_{23}$ OH). Precise amounts used in the formulation can be found in the Experimental Section.

In this study, the TEOVS concentration was kept constant at 2% w/w for experimental simplicity. We do note, however, that the cross-link density of PDMS is adversely affected by the addition of higher concentrations of TEOVS. At [TEOVS] = 5% w/w, it was observed that the final material was significantly softer and readily underwent plastic deformation after 24 h of curing at a temperature of 65 °C. When even higher concentrations of TEOVS were used, the resulting material did not cure into a solid, presumably due to the consumption of available cross-linking sites by the silane coupling agent. This effect places a limitation on the Sylgard 184 PDMS recipe, and potentially other similar elastomers, without additional modifications to introduce more cross-linking sites. The exact recipes used in this study have been specified in the Experimental Section.

A 90° peel test setup was used to quantify the interfacial toughness of PAAm hydrogel/PDMS bilayer samples. By peeling off the PDMS from the hydrogel layer affixed to a glass substrate, traces of the peeling force against peeling extension were obtained. All tests were initiated by making a precrack of less than 5 mm using a razor blade and were performed at a constant peeling rate of 50 mm/min over a length of at least 60 mm. When the crack propagates through the bilayer, the peeling force eventually settles into a steady-state regime. The strain energy release rate during peeling, G, is given by[54] $G = F/b(1 - \cos\theta)$ for peel angle θ, peel force F, and sample width b. This expression simplifies to $G = F/b$ for $\theta = 90°$. Under steady-state crack propagation, the interfacial fracture energy or toughness Γ is equal to the energy release rate G, so that Γ is given by the measured plateau peeling force divided by the width of the specimen.

RESULTS AND DISCUSSION

The peeling tests reveal clear differences in adhesive behavior depending on the compositions that are used in the hydrogel and elastomer. In all of the discussed tests, the silane concentration in the PDMS was kept constant at 2% w/w of the net PDMS content. As shown in Figure 3, increasing the concentration of the coupling agent corresponds to an increase in the adhesive strength of the interface. However, this trend only holds for cases where the surfactant is incorporated into the PDMS (1% BrijL23 condition). Within these conditions, the highest interfacial toughness achieved was $\Gamma = 84.74 \pm 2.25$ J/m^2 at [TMSPMA] = 30.4 μL/mL and 1% BrijL23.

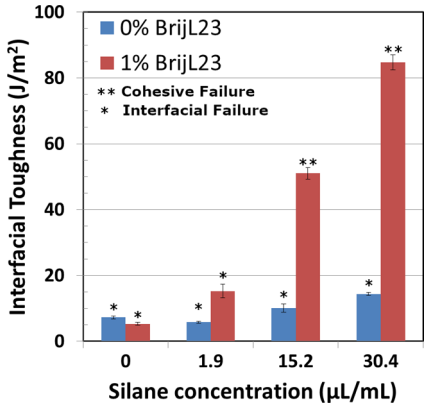

Figure 3. Cast hydrogel−PDMS bilayers with varying hydrogel silane concentrations (TMSPMA) and PDMS surfactant contents (BrijL23). The PDMS silane concentration (TEOVS) was kept constant at 2% w/w relative to the PDMS mass. It is evident that the presence of both surfactant and silane are required to obtain good adhesion. We note that a transition from interfacial failure to cohesive failure was observed at 15.2 μL/mL of TMSPMA for the 1% BrijL23 condition.

For samples with surfactant, experimental observations indicate that a transition from interfacial failure at the PAAm−PDMS interface to cohesive failure through the PAAm hydrogel occurs around [TMSPMA] = 15.2 μL/mL, as permanent damage can be seen in the hydrogel after peeling and solid residues remain on the PDMS. The fingering instabilities that form during peeling (see the Supporting Information Figure S2) begin to form clearly defined ligaments with more silane coupling agent (Supporting Information Figures S2 and S3). This behavior is consistent with previous studies of soft material adhesion[41] and may be attributed to either elastic[55−57] or viscoelastic effects in the adhesive.[58] These instabilities remain temporarily after peeling for the lower silane concentrations and are permanent for the higher concentrations (above [TMSPMA] = 15.2 μL/mL). Previous studies have indicated that some mechanisms allow for the participation of the rheological modifier in the formation of these peeling instabilities.[41] These mechanisms require a degree of hydrophilicity of the PDMS surface, which indeed occurs in this system when the surfactant is introduced. Further investigation is required to establish whether the rheological modifier plays an equivalent role here.

It is expected that the positive correlation between TMSPMA and interfacial toughness (Figure 3) continues above the tested range of TMSPMA. Experiments with hydrogel precursors containing [TMSPMA] = 60.8 μL/mL resulted in a phase-separated mixture that was impossible to

https://dx.doi.org/10.1021/acsami.0c07468
ACS Appl. Mater. Interfaces 2020, 12, 31002−31009

UV cure under standard conditions. TMSPMA was still incorporated into the gel mixture, as the hydrogel cross-links via self-condensation of the silane over the course of several days. This observation suggests that the UV initiator is affected by the TMSPMA. Even so, observations for the 1% BrijL23 and [TMSPMA] = 30.4 μL/mL condition suggest that the interfacial toughness is bounded by the toughness of the hydrogel rather than the hydrogel−PDMS interface. Modifying the hydrogel recipe by halving the amount of UV cross-linker (corresponding to the *N*,*N*′-methylenebis(acrylamide) or MBAA) and keeping all other factors constant resulted in a stronger interface with peak peeling forces indicating G = 127 J/m^2. According to the Lake−Thomas model,[59] reducing the cross-linking density of the hydrogel network leads to a greater capacity for elastic energy dissipation. This increase in energy dissipation would lead to a corresponding increase to the overall interfacial toughness, provided the internetwork bonding is of sufficient strength to allow for such deformation.[46] Thus, further improvements to the interfacial toughness will likely need to include toughening mechanisms for the materials being printed. Since it is well known that the TMSPMA acts as a secondary cross-linker within the hydrogel, designing materials should factor in the ultimate material properties after both the standard copolymerization process and the coupling reactions have occurred.[38] We note that unless the pH is modified to an alkaline environment, complete condensation will likely take a significant period of time due to coupling kinetics.[49]

In the condition where no surfactant was used (0% BrijL23), minimal changes were observed in the peeling behavior with increasing [TMSPMA]. Fingering instabilities were present as soon as TMSPMA was introduced, in line with the 1% BrijL23 and [TMSPMA] = 1.9 μL/mL condition, but only interfacial failure was observed for the entire range of surfactant/silane explored. This suggests that the surfactant is a necessary mediator of the coupling reaction for the range of compositions explored. This finding is in stark contrast with previous experiments that demonstrated that surfactant is not necessary for satisfactory hydrogel−elastomer bonding outside of a printing-relevant context.[38] In these experiments, strong adhesion was obtained even in the absence of the surfactant. Clearly, incorporating the rheological modifier into the precursors to make them suitable for extrusion printing has a more profound effect than just changing their viscosity. To investigate this, we examined all components and processing steps that differ between Liu et al.[38] and the present system. This investigation has led to the conclusion that the presence of the rheological modifier has a detrimental effect on the final adhesive strength that can be attained, even though the mechanism by which this happens is not understood. The effect has been observed even for reduced concentrations of the rheological modifier, down to 25% of the quantities reported in the Experimental Section.

It was initially suspected that using centrifugal instead of vortex mixing exhausted silanol sites prior to interfacial condensation. Although the rheological modifier is too viscous to mix using a vortex mixer and centrifugal mixing must be used, testing indicates that there is no appreciable difference between the two processing techniques (Supporting Information Figure S4). Hydrogel precursor formulations that do not utilize any rheological modifier achieve similar levels of adhesion and are all observed to experience cohesive failure. Inserting a waiting time at room temperature does little to affect the adhesive strength, and additional tests verified that inserting a waiting time at elevated temperatures of 65 °C also has minimal effect. Mixture temperatures during centrifugal mixing were observed to be elevated up to 41−45 °C, with the rheological modifier contributing to a 4 °C increase in steady-state temperature during mixing; this was too small of a difference to warrant further consideration. Several other possible explanations for this effect were explored, but none yielded a concrete mechanism. One obvious factor is the precursor viscosity, where the high viscosity required for printing may adversely affect the kinetics of condensation. Though this appears consistent with observations, internal tests and previous work[38] without the PAAm rheological modifier both showed that cohesive failure can be obtained by having fully cured hydrogel and PDMS making contact at elevated temperatures. A solid network is a sufficiently close approximation to a liquid with near-infinite viscosity that the hypothesis appears to fail by an experimental *reductio ad absurdum*. Another possible mechanism is an interaction between the monomer (acrylamide) and the silane coupling agent. Repeated internal tests confirmed, however, that cohesive failure was still achieved with hydrogel precursors of the equivalent network monomer content as monomer and rheological modifier combined. While we were unable to determine the precise mechanism, it is evident from the experiments that the addition of the rheological modifier necessitates significantly more TMSPMA and the presence of a surfactant to achieve good interfacial toughness of the hydrogel−PDMS interface.

To explore the effects of the surfactant concentration on the adhesive strength, we maintained a constant concentration of the TMSPMA ([TMSPMA] = 30.4 μL/mL) and varied the surfactant concentration (BrijL23) in the PDMS. Figure 4 shows that there is an optimal amount of surfactant, which occurs approximately at the 1% BrijL23 concentration. Too little surfactant (0.5% and less) leads to interfacial failure, suggesting that an insufficient degree of condensation occurs across the interface in that condition. The low degree of condensation is not due to insufficient hydrolysis given experimental observations of hydrophilicity of the PDMS

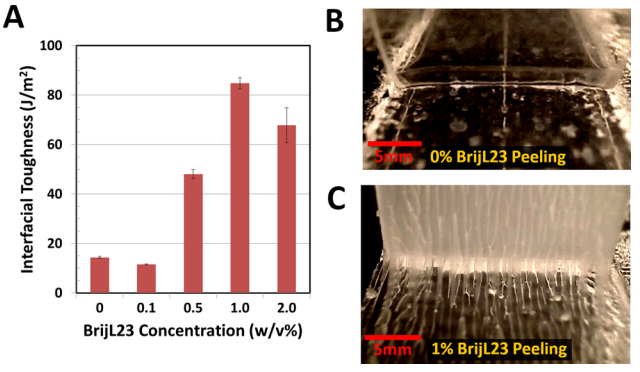

Figure 4. (A) By fixing hydrogel TMSPMA concentration at 30.4 μL/mL and PDMS TEOVS concentration at 2% w/w, we can clearly see the effects of varying the surfactant concentration (BrijL23) on the interfacial toughness. Too little surfactant yields minimal improvement to the adhesion, whereas too much can cause degradation of the adhesion. (B) and (C) Peeling behavior differences between having 0 and 1% surfactant, which shows interfacial and hydrogel cohesive failure, respectively.

https://dx.doi.org/10.1021/acsami.0c07468
ACS Appl. Mater. Interfaces 2020, 12, 31002−31009

surfaces. Both with and without surfactant, the PDMS surfaces showed hydrophilic wetting behavior after peeling and DI water rinsing, even when no cohesive failure was observed. Prior to contact with the hydrogel precursor, however, the PDMS was hydrophobic in all cases. These observations suggest that hydrolysis of the TEOVS occurs in the time that the PDMS is in contact with the PAAm hydrogel, irrespective of the presence of the surfactant. This hypothesis is also supported by previous reports that silane surface-mediated hydrolysis only occurs upon contact with water.[38] Too much surfactant (2% BrijL23), on the other hand, still yields cohesive failures, but the adhesive energy is lower than at 1% BrijL23. These results are consistent with previously reported results that hypothesized higher surfactant concentrations lead to crowding out of the silane functional groups at the interface.[38] While our results do not shed further light on the precise mechanism, they do confirm the general trend of a local maximum of effectiveness for surfactant action.

To validate these results obtained using cast bulk material, samples were also fabricated using extrusion printing.[40] As illustrated in Figure 5A, a 500 μm barrel was used to extrude a

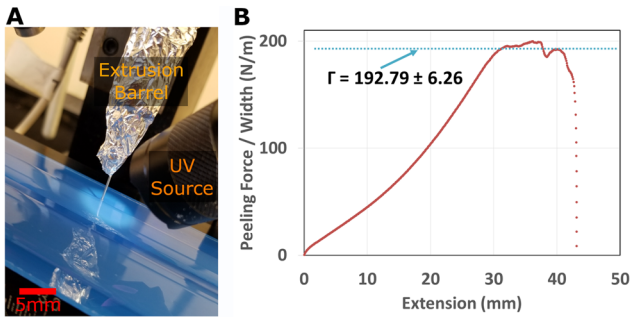

Figure 5. (A) Samples are fabricated via material extrusion from a syringe barrel (wrapped in an aluminum foil) in a customized extrusion printing machine for the peeling test shown in (B). PDMS was printed first and cured to completion prior to hydrogel extrusion. Both hydrogel and PDMS were printed as a 20 mm × 70 mm sheet with a 500 μm inner-diameter syringe tip. (B) Peeling tests indicate good adhesion with failure primarily within the bulk hydrogel near the hydrogel−glass interface rather than at the hydrogel−PDMS interface.

UV-curable formulation of PDMS, which was then fully cured prior to extrusion of the hydrogel precursor directly on top. A glass plate was placed on top of the hydrogel precursor using spacers prior to a complete UV cure within a nitrogen purged container to provide for a rigid peeling substrate with a strong bonding to the hydrogel. A peeling test was then performed using printed bilayer sheets of PAAm−PDMS (Figure 5B), which showed good bonding between hydrogel and PDMS elastomer with $\Gamma = 192.8 \pm 6.3$ J/m^2. It is worth noting that, based on the presence of hydrophilic residues present on the glass surface, the failure occurred primarily within the hydrogel bulk near the hydrogel−glass rather than the hydrogel−PDMS interface, despite an initial crack at the hydrogel−PDMS interface (Supporting Information Figure S5), suggesting that the measured value is a lower bound for the actual interfacial toughness.

CONCLUSIONS

In summary, we have successfully demonstrated that, with the appropriate modifications, a silane coupling agent strategy is viable for the extrusion printing of hydrogel onto PDMS elastomer. Although the condensation reaction is inhibited due to the presence of the rheological modifier in the hydrogel precursor, the combination of a noncharged surfactant and increased concentration of coupling agent is sufficient to overcome this issue, resulting in cohesive rather than adhesive failure. Our experiments suggest that the interfacial adhesion is bounded by the bulk material toughness and not the interfacial toughness. Thus, further enhancements to the adhesion must include mechanical toughening mechanisms for the hydrogel and PDMS materials. Although further work needs to be done to establish full compatibility of the coupling agent strategy for the extrusion printing of elastomers on top of high ionic strength hydrogels, this work serves as an important step in verifying the potential of silanes to serve well in this task.

EXPERIMENTAL SECTION

Preparation of the Thermal-Curing PDMS. The Sylgard 184 (Dow Corning) silicone elastomer kit, consisting of a two-part precursor for base and curing agent, was used as provided. The base was prepared by first mixing in varying amounts of BrijL23 (Sigma-Aldrich, P1254) and triethoxyvinylsilane (TEOVS, Sigma-Aldrich, 175560) via a planetary centrifugal mixer (Thinky, ThinkyMixer ARE-300) for 10 min at 2000 rpm. The resulting mixture was then allowed to cool for 10 min prior to mixing with the curing agent at the prescribed 10:1 ratio for 90 s at 2000 rpm. The TEOVS content was fixed to 2% w/w relative to the net weight of base and curing agent. BrijL23 was varied as a weight percentage of the net weight of base and curing agent. Casting was performed using a 20 mm × 70 mm × 1.6 mm acrylic mold, followed by degassing for 30 min at 70 kPa vacuum. The degassed PDMS was then sealed by applying pressure with a glass plate and cured at 65 °C for 18 h.

Preparation of the UV-Curable PDMS. A UV-curable formulation of PDMS elastomer (Shin-Etsu Silicones, KER-4690 A/B) was provided by the manufacturer as a two-part precursor and was used in the recommended 1:1 ratio. Part A was first mixed with BrijL23 and TEOVS for 10 min at 2000 rpm, as described for thermal-curing PDMS, and then allowed to cool for 10 min. The resulting mixture was then mixed with part B for 90 s at 2000 rpm and used for extrusion printing immediately. Extrusion printing involved nozzle extrusion and exposure to 365 nm UV at a dose rate of 5 mW/cm^2. The material was flood cured using 365 nm UV light at a dose of 35 mW/cm^2 for a period of 90 min and then baked at 65 °C for 18 h.

Preparation of Hydrogel. The hydrogel precursor consisted of acrylamide (AAm, Sigma-Aldrich, A8887), 2-hydroxy-4′-(2-hydroxyethoxy)-2-methylpropiophenone (Irgacure 2959, Sigma-Aldrich, 410896), *N*,*N*,*N*′,*N*′-tetramethylethylenediamine (TEMED, Sigma-Aldrich, T7024), *N*,*N*′-methylenebis(acrylamide) (MBAA, Sigma-Aldrich, 146072), 3-(trimethoxysilyl)propylmethacrylate (TMSPMA, Sigma-Aldrich, 440159), acetic acid (Sigma-Aldrich, A6283), and lithium chloride (LiCl, Sigma-Aldrich, 62476) dissolved in either DI water or a polyacrylamide (PAAm) solution. Irgacure 2959 was dissolved in ethanol (459836, Sigma-Aldrich) to facilitate dissolution and transfer. TMSPMA concentration is specified in this study as a volume concentration relative to the rheological modifier solution (or DI water) volume. Mixing was performed using a planetary centrifugal mixer (Thinky, ThinkyMixer ARE-300). The PAAm solution was synthesized by UV exposure of a solution containing AAm and Irgacure 2959 at a dose rate of 35 mW/cm^2 at 365 nm for 50 min. The PAAm solution precursor used a mass ratio of 92.52% deionized water (resistivity = 18.2 MΩ cm), 7.402% AAm, 0.002075% Irgacure 2959, and 0.07302% ethanol.

The final mass ratios for the hydrogel precursor with the PAAm rheological modifier and [TMSPMA] = 30.4 μL/mL were 62.67% DI water, 4.891% PAAm, 9.172% AAm, 21.30% LiCl, 0.01834% MBAA, 0.002742% Irgacure 2959, 1.9417% TMSPMA, and 0.0037% acetic acid. All hydrogel precursors were exposed to a 15 W bench UV Lamp (XX-15, UVP), at a distance of 1 cm yielding an average dose rate of 30 mW/cm^2 at 365 nm for 50 min.

https://dx.doi.org/10.1021/acsami.0c07468
ACS Appl. Mater. Interfaces 2020, 12, 31002−31009

PDMS−Hydrogel Bilayer Preparation. For cast experiments, PDMS segments were placed within an acrylic mold to allow for the hydrogel precursor to be cast directly on top of the PDMS. The molds were subsequently sealed within a polypropylene container. The container was then purged with nitrogen gas bubbled through a saturated salt solution of potassium carbonate, yielding a relative humidity (RH) of 43%; this step displaces oxygen but maintains a stable RH for successful free radical polymerization of the hydrogel. The hydrogel precursor was then cured via UV exposure while in contact with a glass plate, which led to the adhesion of the glass to the hydrogel without additional modifications. Afterward, the bilayers were baked in an oven at 65 °C for 24 h prior to testing. Pressure was applied directly to the PDMS during mold removal to maintain the integrity of the interface for testing. Printed bilayers underwent similar steps, though casting was replaced by extrusion printing for both PDMS and hydrogel by the customized milling machine described in ref 40.

To rule out effects of humidity during synthesis of the hydrogel precursor, TMSPMA was also prehydrolyzed prior to addition to the rest of the hydrogel precursor by vortex mixing it with an acidic aqueous solution (pH = 3.0, acetic acid) for 10 min. Hydrolysis of TMSPMA did not induce any change to the adhesion with rheological modifier present. Regarding PDMS processing, modifying the mixing order of its components (base, surfactant, silane, and curing agent) did not cause significant changes in the results.

Mechanical Characterizations. Peeling tests were performed on a dual-column mechanical tester (Instron, 5966), with 100 N load cell (Instron, 2530-100N) and 90° peel test fixture (Instron, 2820-035) at a constant displacement rate of 50 mm/min. The PDMS portion of the sample was peeled off the hydrogel, with the latter attached to a glass substrate during curing due to silane condensation. Since the PDMS formulation used in this study is relatively stiff with a Young's modulus of ∼2 MPa,[60] a backing layer for the PDMS was not necessary to prevent excessive strains under load. All cast samples were fabricated to be 1.6 mm × 20 mm × 70 mm per material layer and stacked to form a 3.2 mm thick bilayer. A small mechanical clamp was fixed onto one end of the PDMS that allowed for cotton twine to be fed through and thus extend the distance between sample and load cell to minimize the effect of misalignment. Samples were first aligned and then a small initial crack (5 mm) at the front of sample was made. Peeling was then performed for the remainder of the sample, and the interfacial adhesion energy, Γ, was extracted from the steady-state region of the peeling force.

■ ASSOCIATED CONTENT

Supporting Information

The Supporting Information is available free of charge at https://pubs.acs.org/doi/10.1021/acsami.0c07468.

Rheological modifier and additional experimental observations have been compiled in a docx (PDF)

■ AUTHOR INFORMATION

Corresponding Authors

Zhigang Suo − *Harvard School of Engineering and Applied Sciences and Kavli Institute for Bionano Science and Technology, Harvard University, Cambridge, Massachusetts 02138, United States;* orcid.org/0000-0002-4068-4844; Email: suo@seas.harvard.edu

Joost J. Vlassak − *Harvard School of Engineering and Applied Sciences, Harvard University, Cambridge, Massachusetts 02138, United States*; Email: vlassak@seas.harvard.edu

Author

Kevin Tian − *Harvard School of Engineering and Applied Sciences, Harvard University, Cambridge, Massachusetts 02138, United States;* orcid.org/0000-0003-4821-4959

Complete contact information is available at: https://pubs.acs.org/10.1021/acsami.0c07468

Author Contributions

The study was jointly designed by K.T., Z.S., and J.J.V., and executed by K.T. The manuscript was written through contributions of all authors. All authors have given approval of the final version of the manuscript.

Funding

This research was supported by NSF (CMMI-1404653) and by the Harvard University MRSEC via NSF (DMR-1420570). Part of this work was performed at facilities supported by NSF (ECS 1541959).

Notes

The authors declare no competing financial interest.

■ ABBREVIATIONS USED

PDMS, poly(dimethylsiloxane)
AAm, acrylamide
PAAm, polyacrylamide
LiCl, lithium chloride
RH, relative humidity
TMSPMA, 3-(tri-methoxy-silyl)propylmethacrylate
TEOVS, tri-ethoxy-vinylsilane

■ REFERENCES

(1) Yang, C.; Suo, Z. Hydrogel Ionotronics. *Nat. Rev. Mater.* **2018**, *3*, 125−142.

(2) Sun, J.-Y.; Keplinger, C.; Whitesides, G. M.; Suo, Z. Ionic Skin. *Adv. Mater.* **2014**, *26*, 7608−7614.

(3) Larson, C.; Peele, B.; Li, S.; Robinson, S.; Totaro, M.; Beccai, L.; Mazzolai, B.; Shepherd, R. Highly Stretchable Electroluminescent Skin for Optical Signaling and Tactile Sensing. *Science* **2016**, *351*, 1071−1074.

(4) Kim, D.-H.; Lu, N.; Ma, R.; Kim, Y.-S.; Kim, R.-H.; Wang, S.; Wu, J.; Won, S. M.; Tao, H.; Islam, A.; Yu, K. J.; Kim, T. T. -i.; Chowdhury, R.; Ying, M.; Xu, L.; Li, M.; Chung, H.-J.; Keum, H.; McCormick, M.; Liu, P.; Zhang, Y.-W.; Omenetto, F. G.; Huang, Y.; Coleman, T.; Rogers, J. A. Epidermal Electronics. *Science* **2011**, *333*, 838−843.

(5) Yuk, H.; Zhang, T.; Parada, G. A.; Liu, X.; Zhao, X. Skin-Inspired Hydrogel−Elastomer Hybrids with Robust Interfaces and Functional Microstructures. *Nat. Commun.* **2016**, *7*, No. 12028.

(6) Yang, C. H.; Chen, B.; Lu, J. J.; Yang, J. H.; Zhou, J.; Chen, Y. M.; Suo, Z. Ionic Cable. *Extrem. Mech. Lett.* **2015**, *3*, 59−65.

(7) Guo, J.; Liu, X.; Jiang, N.; Yetisen, A. K.; Yuk, H.; Yang, C.; Khademhosseini, A.; Zhao, X.; Yun, S.-H. Highly Stretchable, Strain Sensing Hydrogel Optical Fibers. *Adv. Mater.* **2016**, *28*, 10244−10249.

(8) Kim, C.-C.; Lee, H.-H.; Oh, K. H.; Sun, J.-Y. Highly Stretchable, Transparent Ionic Touch Panel. *Science* **2016**, *353*, 682−687.

(9) Chen, C. H.; Pun, S. H.; Mak, P. U.; Vai, M. I.; Klug, A.; Lei, T. C. Circuit Models and Experimental Noise Measurements of Micropipette Amplifiers for Extracellular Neural Recordings from Live Animals. *Biomed Res. Int.* **2014**, *2014*, No. 135026.

(10) Yang, C. H.; Chen, B.; Zhou, J.; Chen, Y. M.; Suo, Z. Electroluminescence of Giant Stretchability. *Adv. Mater.* **2016**, *28*, 4480−4484.

(11) Manandhar, P.; Calvert, P. D.; Buck, J. R. Elastomeric Ionic Hydrogel Sensor for Large Strains. *IEEE Sens. J.* **2012**, *12*, 2052−2061.

(12) Le Floch, P.; Yao, X.; Liu, Q.; Wang, Z.; Nian, G.; Sun, Y.; Jia, L.; Suo, Z. Wearable and Washable Conductors for Active Textiles. *ACS Appl. Mater. Interfaces* **2017**, *9*, 25542−25552.

(13) Han, D.; Lu, Z.; Chester, S. A.; Lee, H. Micro 3D Printing of a Temperature-Responsive Hydrogel Using Projection Micro-Stereolithography. *Sci. Rep.* **2018**, *8*, No. 1963.
(14) Xing, J.-F.; Zheng, M.-L.; Duan, X.-M. Two-Photon Polymerization Microfabrication of Hydrogels: An Advanced 3D Printing Technology for Tissue Engineering and Drug Delivery. *Chem. Soc. Rev.* **2015**, *44*, 5031−5039.
(15) Li, L.; Pan, L.; Ma, Z.; Yan, K.; Cheng, W.; Shi, Y.; Yu, G. All Inkjet-Printed Amperometric Multiplexed Biosensors Based on Nanostructured Conductive Hydrogel Electrodes. *Nano Lett.* **2018**, *18*, 3322−3327.
(16) Negro, A.; Cherbuin, T.; Lutolf, M. P. 3D Inkjet Printing of Complex, Cell-Laden Hydrogel Structures. *Sci. Rep.* **2018**, *8*, No. 17099.
(17) Bakarich, S. E.; Gorkin, R.; Panhuis, M.; Spinks, G. M. Three-Dimensional Printing Fiber Reinforced Hydrogel Composites. *ACS Appl. Mater. Interfaces* **2014**, *6*, 15998−16006.
(18) Landers, R.; Hübner, U.; Schmelzeisen, R.; Mülhaupt, R. Rapid Prototyping of Scaffolds Derived from Thermoreversible Hydrogels and Tailored for Applications in Tissue Engineering. *Biomaterials* **2002**, *23*, 4437−4447.
(19) Lewis, J. A. Direct Ink Writing of 3D Functional Materials. *Adv. Funct. Mater.* **2006**, *16*, 2193−2204.
(20) Rundle, G. *A Revolution in the Making: 3D Printing, Robots and the Future*; Affirm Press: South Melbourne, Victoria Australia, 2014.
(21) Bakarich, S. E.; Panhuis, M.; Beirne, S.; Wallace, G. G.; Spinks, G. M. Extrusion Printing of Ionic−Covalent Entanglement Hydrogels with High Toughness. *J. Mater. Chem. B* **2013**, *1*, 4939−4946.
(22) Hanson Shepherd, J. N.; Parker, S. T.; Shepherd, R. F.; Gillette, M. U.; Lewis, J. A.; Nuzzo, R. G. 3D Microperiodic Hydrogel Scaffolds for Robust Neuronal Cultures. *Adv. Funct. Mater.* **2011**, *21*, 47−54.
(23) Barry, R. A.; Shepherd, R. F.; Hanson, J. N.; Nuzzo, R. G.; Wiltzius, P.; Lewis, J. A. Direct-Write Assembly of 3D Hydrogel Scaffolds for Guided Cell Growth. *Adv. Mater.* **2009**, *21*, 2407−2410.
(24) Du, Q.; Tang, Q.; Yang, K.; Yang, H.; Xu, C.; Zhang, X. One-Step Preparation of Tough and Self-Healing Polyion Complex Hydrogels with Tunable Swelling Behaviors. *Macromol. Rapid Commun.* **2019**, *40*, No. 1800691.
(25) Luo, F.; Sun, T. L.; Nakajima, T.; Kurokawa, T.; Zhao, Y.; Sato, K.; Ihsan, A. B.; Li, X.; Guo, H.; Gong, J. P. Oppositely Charged Polyelectrolytes Form Tough, Self-Healing, and Rebuildable Hydrogels. *Adv. Mater.* **2015**, *27*, 2722−2727.
(26) Dou, P.; Liu, Z.; Cao, Z.; Zheng, J.; Wang, C.; Xu, X. Rapid Synthesis of Hierarchical Nanostructured Polyaniline Hydrogel for High Power Density Energy Storage Application and Three-Dimensional Multilayers Printing. *J. Mater. Sci.* **2016**, *51*, 4274−4282.
(27) Luo, F.; Sun, T. L.; Nakajima, T.; King, D. R.; Kurokawa, T.; Zhao, Y.; Ihsan, A. B.; Li, X.; Guo, H.; Gong, J. P. Strong and Tough Polyion-Complex Hydrogels from Oppositely Charged Polyelectrolytes: A Comparative Study with Polyampholyte Hydrogels. *Macromolecules* **2016**, *49*, 2750−2760.
(28) Zhu, F.; Cheng, L.; Yin, J.; Wu, Z. L.; Qian, J.; Fu, J.; Zheng, Q. 3D Printing of Ultratough Polyion Complex Hydrogels. *ACS Appl. Mater. Interfaces* **2016**, *8*, 31304−31310.
(29) Muth, J. T.; Vogt, D. M.; Truby, R. L.; Mengüç, Y.; Kolesky, D. B.; Wood, R. J.; Lewis, J. A. Embedded 3D Printing of Strain Sensors within Highly Stretchable Elastomers. *Adv. Mater.* **2014**, *26*, 6307−6312.
(30) Frutiger, A.; Muth, J. T.; Vogt, D. M.; Mengüç, Y.; Campo, A.; Valentine, A. D.; Walsh, C. J.; Lewis, J. A. Capacitive Soft Strain Sensors via Multicore-Shell Fiber Printing. *Adv. Mater.* **2015**, *27*, 2440−2446.
(31) Hardin, J. O.; Ober, T. J.; Valentine, A. D.; Lewis, J. A. Microfluidic Printheads for Multimaterial 3D Printing of Viscoelastic Inks. *Adv. Mater.* **2015**, *27*, 3279−3284.
(32) Hinton, T. J.; Hudson, A.; Pusch, K.; Lee, A.; Feinberg, A. W. 3D Printing PDMS Elastomer in a Hydrophilic Support Bath via Freeform Reversible Embedding. *ACS Biomater. Sci. Eng.* **2016**, *2*, 1781−1786.
(33) Truby, R. L.; Lewis, J. A. Printing Soft Matter in Three Dimensions. *Nature* **2016**, *540*, 371−378.
(34) Gerratt, A. P.; Michaud, H. O.; Lacour, S. P. Elastomeric Electronic Skin for Prosthetic Tactile Sensation. *Adv. Funct. Mater.* **2015**, *25*, 2287−2295.
(35) Hung, K.-C.; Tseng, C.-S.; Hsu, S.-h. Synthesis and 3D Printing of Biodegradable Polyurethane Elastomer by a Water-Based Process for Cartilage Tissue Engineering Applications. *Adv. Healthcare Mater.* **2014**, *3*, 1578−1587.
(36) Roh, S.; Parekh, D. P.; Bharti, B.; Stoyanov, S. D.; Velev, O. D. 3D Printing by Multiphase Silicone/Water Capillary Inks. *Adv. Mater.* **2017**, *29*, No. 1701554.
(37) Yang, H.; Li, C.; Yang, M.; Pan, Y.; Yin, Q.; Tang, J.; Qi, H. J.; Suo, Z. Printing Hydrogels and Elastomers in Arbitrary Sequence with Strong Adhesion. *Adv. Funct. Mater.* **2019**, *1901721*, No. 1901721.
(38) Liu, Q.; Nian, G.; Yang, C.; Qu, S.; Suo, Z. Bonding Dissimilar Polymer Networks in Various Manufacturing Processes. *Nat. Commun.* **2018**, *9*, No. 846.
(39) Robinson, S. S.; O'Brien, K. W.; Zhao, H.; Peele, B. N.; Larson, C. M.; Mac Murray, B. C.; Van Meerbeek, I. M.; Dunham, S. N.; Shepherd, R. F. Integrated Soft Sensors and Elastomeric Actuators for Tactile Machines with Kinesthetic Sense. *Extrem. Mech. Lett.* **2015**, *5*, 47−53.
(40) Tian, K.; Bae, J.; Bakarich, S. E.; Yang, C.; Gately, R. D.; Spinks, G. M.; Panhuis, M.; Suo, Z.; Vlassak, J. J. 3D Printing of Transparent and Conductive Heterogeneous Hydrogel-Elastomer Systems. *Adv. Mater.* **2017**, *29*, No. 1604827.
(41) Tian, K.; Bae, J.; Suo, Z.; Vlassak, J. J. Adhesion between Hydrophobic Elastomer and Hydrogel through Hydrophilic Modification and Interfacial Segregation. *ACS Appl. Mater. Interfaces* **2018**, *10*, 43252−43261.
(42) Darabi, M. A.; Khosrozadeh, A.; Mbeleck, R.; Liu, Y.; Chang, Q.; Jiang, J.; Cai, J.; Wang, Q.; Luo, G.; Xing, M. Skin-Inspired Multifunctional Autonomic-Intrinsic Conductive Self-Healing Hydrogels with Pressure Sensitivity, Stretchability, and 3D Printability. *Adv. Mater.* **2017**, *29*, No. 1700533.
(43) Wehner, M.; Truby, R. L.; Fitzgerald, D. J.; Mosadegh, B.; Whitesides, G. M.; Lewis, J. A.; Wood, R. J. An Integrated Design and Fabrication Strategy for Entirely Soft, Autonomous Robots. *Nature* **2016**, *536*, 451−455.
(44) Lin, S.; Yuk, H.; Zhang, T.; Parada, G. A.; Koo, H.; Yu, C.; Zhao, X. Stretchable Hydrogel Electronics and Devices. *Adv. Mater.* **2016**, *28*, 4497−4505.
(45) Parada, G. A.; Yuk, H.; Liu, X.; Hsieh, A. J.; Zhao, X. Impermeable Robust Hydrogels via Hybrid Lamination. *Adv. Healthcare Mater.* **2017**, *6*, No. 1700520.
(46) Yuk, H.; Zhang, T.; Lin, S.; Parada, G. A.; Zhao, X. Tough Bonding of Hydrogels to Diverse Non-Porous Surfaces. *Nat. Mater.* **2016**, *15*, 190−196.
(47) Plueddemann, E. P. Silane Adhesion Promoters in Coatings. *Prog. Org. Coat.* **1983**, *11*, 297−308.
(48) Witucki, G. L. BACK TO BASICS A Silane Primer: Chemistry and Applications of AIkoxy Silanes. *J. Coat. Technol.* **1993**, *65*, 57−60.
(49) Savard, S.; Blanchard, L.-P.; Léonard, J.; Prud'homme, R. E. Hydrolysis and Condensation of Silanes in Aqueous Solutions. *Polym. Compos.* **1984**, *5*, 242−249.
(50) Wu, Z.; Hjort, K. Surface Modification of PDMS by Gradient-Induced Migration of Embedded Pluronic. *Lab Chip* **2009**, *9*, 1500−1503.
(51) Kim, H. T.; Kim, J. K.; Jeong, O. C. Hydrophilicity of Surfactant-Added Poly(Dimethylsiloxane) and Its Applications. *Jpn. J. Appl. Phys.* **2011**, *50*, No. 06GL04.
(52) Madadi, H.; Casals-Terré, J. Long-Term Behavior of Nonionic Surfactant-Added PDMS for Self-Driven Microchips. *Microsyst. Technol.* **2013**, *19*, 143−150.

https://dx.doi.org/10.1021/acsami.0c07468
ACS Appl. Mater. Interfaces 2020, 12, 31002−31009

(53) Baselga, J.; Llorente, M. A.; Hernández-Fuentes, I.; Piérola, I. F. Polyacrylamide Gels. Process of Network Formation. *Eur. Polym. J.* **1989**, *25*, 477−480.
(54) Creton, C.; Ciccotti, M. Fracture and Adhesion of Soft Materials: A Review. *Rep. Prog. Phys.* **2016**, *79*, No. 046601.
(55) Ghatak, A.; Chaudhury, M. K.; Shenoy, V.; Sharma, A. Meniscus Instability in a Thin Elastic Film. *Phys. Rev. Lett.* **2000**, *85*, 4329−4332.
(56) Adda-Bedia, M.; Mahadevan, L. Crack-Front Instability in a Confined Elastic Film. *Proc. R. Soc. A* **2006**, *462*, 3233−3251.
(57) Villey, R.; Creton, C.; Cortet, P.-P.; Dalbe, M.-J.; Jet, T.; Saintyves, B.; Santucci, S.; Vanel, L.; Yarusso, D. J.; Ciccotti, M. Rate-Dependent Elastic Hysteresis during the Peeling of Pressure Sensitive Adhesives. *Soft Matter* **2015**, *11*, 3480−3491.
(58) Saffman, P. G.; Taylor, G. The Penetration of a Fluid into a Porous Medium or Hele-Shaw Cell Containing a More Viscous Liquid. *Proc. R. Soc. London, Ser. A* **1958**, *245*, 312−329.
(59) Lake, G. J.; Thomas, A. G. The Strength of Highly Elastic Materials. *Proc. R. Soc. London. Ser. A. Math. Phys. Sci.* **1967**, *300*, 108−119.
(60) Johnston, I. D.; McCluskey, D. K.; Tan, C. K. L.; Tracey, M. C. Mechanical Characterization of Bulk Sylgard 184 for Microfluidics and Microengineering. *J. Micromech. Microeng.* **2014**, *24*, No. 035017.

https://dx.doi.org/10.1021/acsami.0c07468
ACS Appl. Mater. Interfaces 2020, 12, 31002−31009